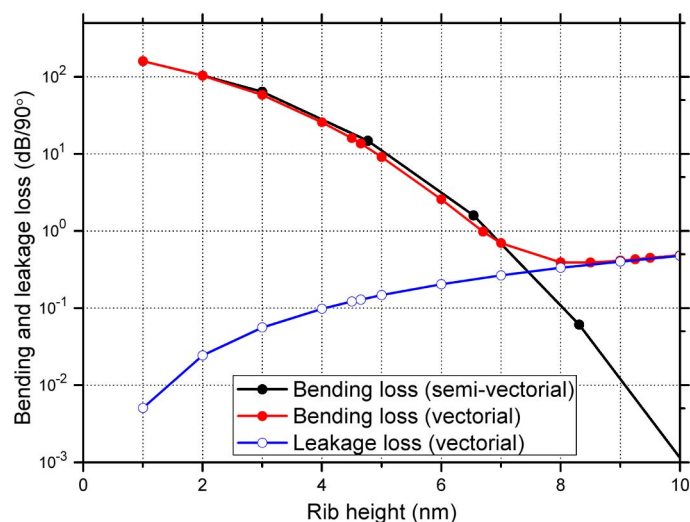


# Single-Mode Limit and Bending Losses for Shallow Rib $\text{Si}_3\text{N}_4$ Waveguides

Volume 7, Number 1, February 2015

Firehun Tsige Dullo  
Jean-Claude Tinguely  
Stian Andre Solbø  
Olav Gaute Hellesø, Member, IEEE



DOI: 10.1109/JPHOT.2014.2387252  
1943-0655 © 2015 IEEE

# Single-Mode Limit and Bending Losses for Shallow Rib Si<sub>3</sub>N<sub>4</sub> Waveguides

Firehun Tsige Dullo,<sup>1</sup> Jean-Claude Tinguely,<sup>2</sup> Stian Andre Solbø,<sup>1</sup> and Olav Gaute Hellesø,<sup>2</sup> *Member, IEEE*

<sup>1</sup>Northern Research Institute, 9294 Tromsø, Norway.

<sup>2</sup>Department of Physics and Technology, University of Tromsø, 9037 Tromsø, Norway.

DOI: 10.1109/JPHOT.2014.2387252

1943-0655 © 2015 IEEE. Translations and content mining are permitted for academic research only.

Personal use is also permitted, but republication/redistribution requires IEEE permission.

See [http://www.ieee.org/publications\\_standards/publications/rights/index.html](http://www.ieee.org/publications_standards/publications/rights/index.html) for more information.

Manuscript received December 4, 2014; revised December 15, 2014; accepted December 16, 2014. Date of publication January 7, 2015; date of current version February 18, 2015. This work was supported by the Research Council of Norway. Corresponding author: F. T. Dullo (e-mail: firehun.tsige.dullo@norut.no).

**Abstract:** The single-mode limit and bending losses for shallow rib waveguides are studied using the full vectorial film mode matching method. The maximum rib height for single-mode waveguides is found to be on the order of 10 nm for a rib width of 2  $\mu\text{m}$  and a wavelength of 785 nm, with the exact value depending on the core thickness and the polarization. Bending losses are calculated as a function of several geometrical parameters, for both polarizations and for the fundamental and the first order modes. Bending losses decrease significantly with rib height for single-mode waveguides. For slightly larger rib heights, giving multimode waveguides, it is found that the bending losses for the first-order mode are several orders of magnitude larger than for the fundamental mode. Thus, a small bend can act as an excellent mode filter, making it possible to use higher ribs giving low bending losses for the fundamental mode, while maintaining the waveguide practically single-mode. For TM-polarization, leakage loss can be important and can cause bending losses to increase for larger rib heights (8–80 nm).

**Index Terms:** Bending loss, single-mode limit, film mode matching method, integrated optics, rib waveguides.

## 1. Introduction

Bending losses are one of the limiting factors for the complexity of integrated optics in general. For waveguide sensors, shallow rib waveguides have recently emerged as attractive due to high sensitivity [1], [2]. However, the small rib height can give high bending losses, as will be shown in this paper. Waveguide sensors offer high sensitivity to a specific physical, chemical or biological parameter [1]–[6]. Most of these devices are based on evanescent field sensing: a subtle change in the refractive index of a layer in contact with the waveguide's evanescent field changes the effective propagation index of the guided mode and thus gives a phase change. These sensors typically require a thin core with high refractive index to maximize the evanescent field and thus obtain high sensitivity [7]. To detect the phase change, the waveguides should be single mode to realize interferometers with high visibility interference. Furthermore, to integrate several sensors and more functions on a chip, it is necessary to have low propagation losses and low bending losses. Shallow rib waveguides are attractive for sensors as they fulfill most of the requirements. High sensitivity is achieved by using a core with a high refractive index (e.g., Si<sub>3</sub>N<sub>4</sub> or Ta<sub>2</sub>O<sub>5</sub>) with a thickness of 60–300 nm. A shallow rib, which is typically 2–10 nm high,

gives single mode operation of rather wide waveguides, e.g., 1–4  $\mu\text{m}$  wide [7]. The low height of the sidewall gives significantly reduced scattering from roughness caused by the etching process during fabrication. Propagation losses are thus reduced [8], [9]. However, for TM-polarization the picture is complicated by leakage loss. The modes of rib-waveguides are hybrid, and the effective refractive index of the fundamental TM-mode (i.e., TM-like) can be lower than the effective index for TE-polarization for the adjacent slab waveguide. This causes leakage loss for TM-polarization as the minority field components leak out [10]–[12]. For both polarizations, the mode confinement decreases as the height of the rib and the sidewall is reduced, causing bending loss to increase. Shallow rib waveguides thus have significantly higher bending losses than normal rib or strip waveguides, and it is necessary to find a compromise between propagation losses and bending losses, with leakage losses also present for TM-polarization.

The fabrication process for shallow rib waveguides is based on silicon technology with deposition of thin films, e.g., with sputtering or chemical vapor deposition (CVD), followed by photolithography and dry etching [13]. During this fabrication process, some geometrical parameters can be precisely set, while others will have significant variation from batch to batch and even between chips from the same wafer. The geometrical parameters are core thickness ( $H$ ), rib width ( $W_r$ ) and rib height ( $h_r$ ), and, for bends, the bend radius ( $R$ ). The bend radius is precisely fixed by photolithography. That is also the case for the rib width, although it will change somewhat during fabrication. A deposition process determines the core thickness, and some variation can be expected. The most difficult parameter to set is the shallow rib height. A variation of 1–2 nm can be expected from one wafer to the next, representing a variation of up to 50% of the height. As will be shown, the leakage loss and the bending loss depend strongly on the rib height. During the design process, it is thus important to take the rib height variation into account and to know its influence on the performance of the device.

For waveguide sensors, a common design criterion is to have minimal bending losses while keeping the waveguide single mode. Before considering bending losses, we thus find the values of the geometrical parameters that ensure single mode waveguides. For this, we have used the full vectorial mode matching method (FMM) [10]. Subsequently, we use the same method to find the dependency of the leakage losses and the bending losses on the geometrical parameters. The results provide necessary information for the design of waveguide devices using shallow rib waveguides. Particular attention is given to the variation in performance with rib height. Previous works have investigated waveguides with relatively thick ribs, finding the maximum rib height giving single-mode waveguides [14], [15] and calculating the bending losses [16], [17]. The rib heights considered in this paper are on the order of 10 nm, which have not been investigated previously regarding bending losses. Polarization can influence the bending losses considerably and leakage losses are only present for TM-polarization. We have thus done simulations for both TE- and TM-polarization regarding several parameters. It is most common to simulate bending losses for the fundamental mode only. However, a waveguide might become multimode due to fabrication errors, especially for the small rib heights considered here. It is thus of interest to study the bending loss of the first order mode. It will be shown that these can be very high if the waveguide is close to the single-mode limit.

## 2. Waveguide Geometry and Simulation Method

In the simulations we have chosen a waveguide geometry that is suitable for an evanescent field waveguide sensor. The waveguide geometry is shown in Fig. 1. The refractive index of the core is set to  $n_{WG} = 2.05$ , corresponding to silicon nitride, which is commonly used for sensing applications [13], [18].

The refractive index of silica ( $n = 1.46$ ) was used for the substrate ( $n_{sub}$ ) and, if not otherwise noted, for the superstrate ( $n_{sup}$ ) as well. In the simulations, the rib width is  $w_r = 2 \mu\text{m}$  unless otherwise noted. This is a width that can readily be obtained with standard photolithography, while it is narrow enough to give single-mode waveguides, as will be demonstrated. For the wavelength, we have chosen 785 nm as inexpensive diode lasers are available and silicon photodetectors have high

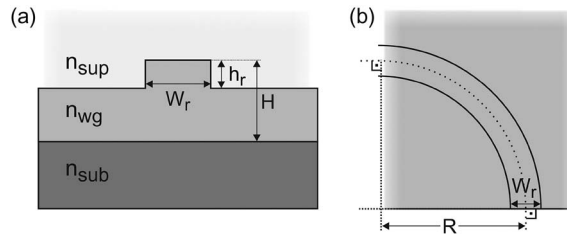


Fig. 1. Geometrical outline of bent shallow rib waveguide showing (a) cross-section and (b) top view.

sensitivity for this wavelength. For sensors, visible and near-infrared wavelengths (i.e., < 1000 nm) are commonly used, rather than the telecommunication wavelengths of 1300 and 1550 nm.

The simulations were performed with the commercial software Fimmwave (Photon Design, Oxford, U.K.). The single-mode limit was found using transparent boundary conditions and full-vectorial calculations, and also using semi-vectorial calculations. The single-mode limit was taken as the largest rib-height  $h_r$  not giving a solution for the first-order mode, for a given core thickness  $H$ , rib width  $W_r$  and polarization. For TE-polarization, the full-vectorial and the semi-vectorial methods give the same results. TM-modes always exhibit leakage loss through the minority field components ( $E_x, H_y$ ). Since the minority field is not included in semi-vectorial calculations, there is a small difference between full-vectorial and semi-vectorial results concerning the single-mode limit. The single-mode limits obtained numerically were also compared to the analytical expressions proposed by Pogossian *et al.* [15].

In order to find the bending losses, we calculated the eigenmodes of bent waveguides using the full-vectorial film mode matching (FMM) method in cylindrical coordinates. In the FMM method, the waveguide cross-section is represented as a series of vertical slices. Each slice corresponds to a multi-layer film structure. The mode profile of the waveguide can be represented as a linear combination of the vertical modes of the different slices; these modes will be either TE- or TM-polarized. The modes in each slice are the solutions of Maxwell's equations. The mode amplitude is obtained using the continuity of the tangential fields at the slice interfaces and the boundary conditions. A two step process was used to find the bending losses, with first finding all the modes of the model (both waveguide and slab modes), with perfectly matched layer (PML) as the boundary condition on both sides of the model. In the second step, the fundamental mode was selected and the complex propagation constant for the mode found. Full-vectorial simulations were used because they consider coupling between the polarizations, which are ignored by semi-vectorial simulations. As noted for straight waveguides, the TM-modes are leaky due to minority field components and, including the minority field components, thus gives more accurate results.

The bending loss  $L$  was found from the simulated imaginary part of the propagation constant  $\beta_i$  and normalized to a 90° bend using

$$L_{90^\circ} = 10\pi R\beta_i \log_{10} e \quad [\text{dB}/90^\circ] \quad (1)$$

with  $R$  as the bend radius. In order to compare the leakage loss with bending loss, the leakage loss was calculated for the length of a 90° bend, i.e.,  $\pi/2 \times R$ .

The simulations were performed with sufficiently high resolution and the results were independent of the model width. In order to verify the model, the single-mode limit and the leakage losses were also calculated for some cases with a different software (Comsol Multiphysics). The two softwares gave almost identical results. Bending losses depend on three geometrical parameters and polarization. However, we have chosen to use 2-D-plots rather than 3-D-plots for clarity. The bending and leakage losses calculated span several decades, and we have used logarithmic scale on the vertical axis of the plots. What appears as a small difference can thus be one order of magnitude.

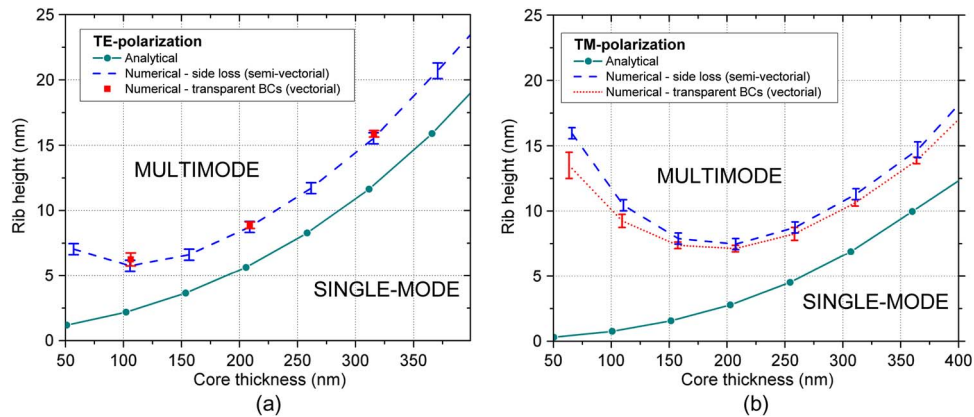


Fig. 2. Limit between single-mode and multimode waveguides as function of core thickness. Results are given for two numerical procedures and according to the analytical expression given by [15]. The rib width is  $2 \mu\text{m}$ . (a) TE-polarization and (b) TM-polarization. The error bars represent the resolution, i.e., the largest rib height that gives a first-order mode and the rib height where such a solution was not found.

### 3. Results and Discussion

Fig. 2 shows the calculated single-mode limit as function of core thickness. For TE-polarization, the two numerical methods (full- and semi-vectorial) give the same results. For TM-polarization, the semi-vectorial method gives slightly different results than the full-vectorial method, as the semi-vectorial method does not consider the minority field components. As the difference is small, we conclude that a semi-vectorial simulation gives a good approximation for these shallow rib waveguides. However, there is a large difference between the numerical results and the analytical approximation. For TE-polarization and large core thicknesses  $H > 250 \text{ nm}$ , the analytical approximation gives a conservative estimate for the single-mode limit, which might be acceptable. For thin cores,  $H < 150 \text{ nm}$ , the discrepancy is so large that the estimate is of no use. For TM-polarization, the analytical estimate is of limited or no value for all the core thicknesses considered here.

A rib height less than  $5 \text{ nm}$  for TE-polarization and less than  $7 \text{ nm}$  for TM-polarization will give single-mode waveguides for all the core thicknesses considered. The minimum values of  $5$  and  $7 \text{ nm}$  are found for core thicknesses of  $110$  and  $210 \text{ nm}$ , for TE- and TM-polarization, respectively. For thicker cores, the single-mode limit increases with increasing core thickness, as predicted also by the analytical expression. For sensing applications, maximum sensitivity is found when the core thickness is approximately  $60 \text{ nm}$  and  $120 \text{ nm}$  for TE and TM polarization, respectively [19]. For these thin cores, the fundamental mode is approaching cut-off for small rib heights, and with the first-order mode necessarily approaching cut-off faster than the fundamental mode, the single-mode limit increases. This effect is particularly relevant for TM-polarization, giving single-mode waveguides for  $10 \text{ nm}$  high ribs for a core thickness of  $100 \text{ nm}$ .

In Fig. 3, the single-mode limit is shown for different superstrate materials: air ( $n_{\text{air}} = 1$ ), water ( $n_{\text{water}} = 1.33$ ), and silica ( $n_{\text{silica}} = 1.46$ ). Except for core thickness  $H = 50 \text{ nm}$ , the influence of the superstrate material on the single-mode limit is small. This is important for devices, including optical sensors, that use different substrate materials along the waveguide, e.g., in the sensing region. The change in substrate material will thus not influence the mode properties of the waveguide, but an abrupt change might cause transition losses, which is outside the scope of this work.

The leakage loss for the fundamental TM mode is shown in Fig. 4. For some specific rib widths, the leakage loss is small for all rib heights. This is due to an interference effect for the minority field component, which cancels the leakage. A thorough treatment of the leakage loss for rib waveguides can be found in [10]. The mode profile for two rib widths, giving high and low

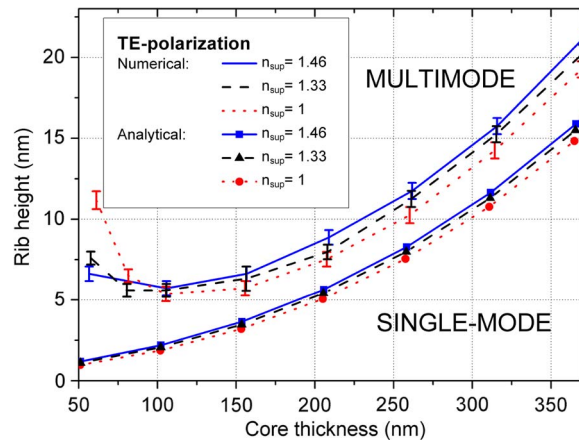


Fig. 3. Influence of the substrate material on the single-mode limit for three substrate materials: air, water, and silica. The numerical results are compared with the analytical expression given by [15]. The rib width is 2  $\mu\text{m}$ , and the results are given for TE-polarization.

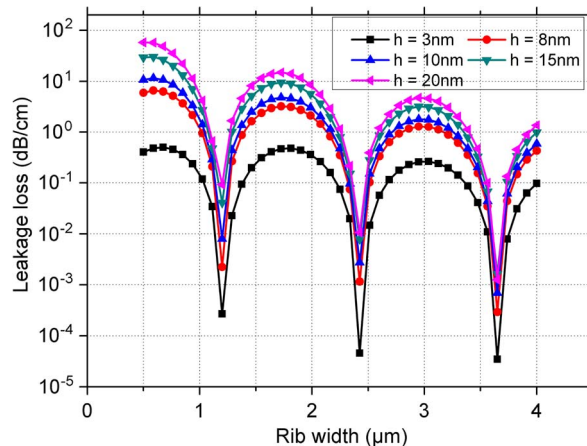


Fig. 4. Leakage loss of the fundamental TM mode versus rib width for five rib heights.

leakage loss respectively, is shown in Fig. 5. The majority field component is in both cases well guided, while the minority field component ( $E_x$ ) is not guided when the leakage loss is high, see Fig. 5(a). A well-guided minority field component is shown in Fig. 5(b) for a rib width which gives cancellation of leakage due to interference. For the rib heights considered in Fig. 4, the leakage loss increases with rib height. This is the case up to a certain rib height, as will be showed when comparing bending and leakage losses.

Bending losses are strongly dependent on the bend radius  $R$ . We start by exploring the dependency on radius, before considering the other geometrical parameters. Fig. 6 shows simulated losses versus radius for TE-polarization and three values of rib width and rib height. All the combinations give single-mode waveguides. The bending losses are exponentially decreasing with radius, and increasing the radius from 1 mm to 3 mm can change the losses with several orders of magnitude. The bending losses decrease with increasing rib width and rib height, as the fundamental mode becomes better guided and the waveguide approaches the limit of becoming multimode. Note that for a rib height of 7 nm and  $R > 3500 \mu\text{m}$ , numerical noise is larger than the bending losses. In the following, we use bend radius  $R = 1 \text{ mm}$  and rib width 2  $\mu\text{m}$  for the simulations. This gives a starting point for choosing geometrical parameters for a waveguide bend, and by going back to Fig. 6, it can be found how the losses change with radius.

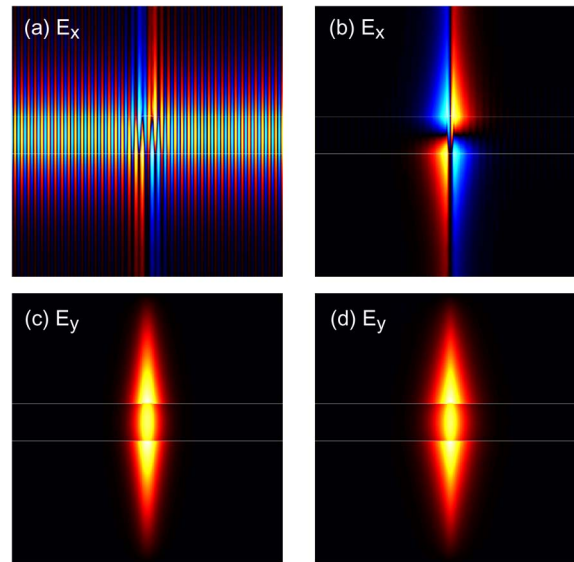


Fig. 5. Field distribution for fundamental, hybrid TM-mode for two rib widths giving (a) large and (b) small leakage loss for the minority field component ( $E_x$ ), while the majority field component ( $E_y$ ) is well guided for both cases [(c) and (d)]. Core thickness 150 nm, rib height 3 nm, rib width  $W_r = 2 \mu\text{m}$  in (a) and (c), and  $W_r = 1.2 \mu\text{m}$  in (b) and (d). The fields are normalized, and a large aspect ratio has been used to show the waveguide thickness.

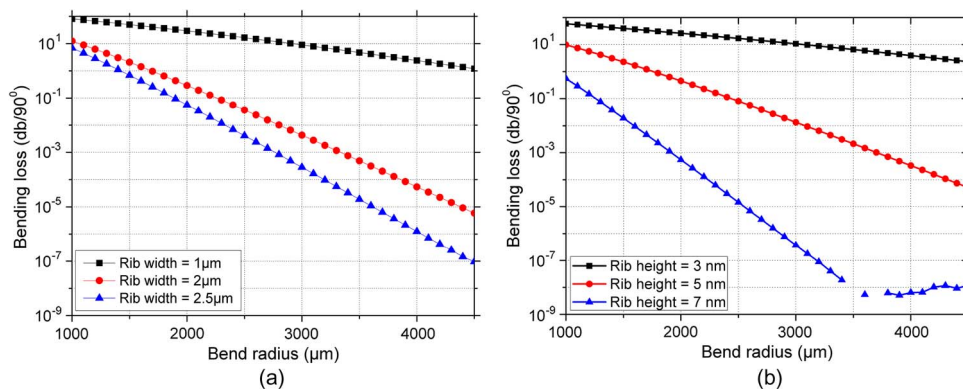


Fig. 6. Bending loss as function of radius and for TE-polarization for (a) three rib widths, with rib height and core thickness fixed to 5 nm and 150 nm, respectively, and for (b) three rib heights, with rib width and core thickness fixed to  $2 \mu\text{m}$  and 150 nm, respectively.

As was shown in Fig. 3, the refractive index of the superstrate has limited influence on the single-mode limit. Fig. 7 shows that the refractive index of the superstrate can change the bending losses with 1–2 orders of magnitude. It is thus necessary to take more precautions when changing the superstrate for a bent waveguide than for a straight waveguide. The bending losses increase with increasing refractive index of the superstrate, which is expected as this gives weaker guiding.

It was shown in Fig. 4 that leakage loss for TM-polarization depends strongly on the rib width and also on the rib height for straight waveguides. It is thus interesting to see how leakage loss contributes to loss in waveguide bends. In Fig. 8, the leakage loss and the bending loss is shown as function of the rib height for a core thickness of 180 nm. The leakage loss is calculated for a straight waveguide with length  $\pi/2 \times R$  and can thus be compared directly with the bending loss for a  $90^\circ$  bend. For small rib heights and thus single-mode waveguides, the bending loss decreases fast with increasing rib height, while the leakage loss increases with rib height. At a rib

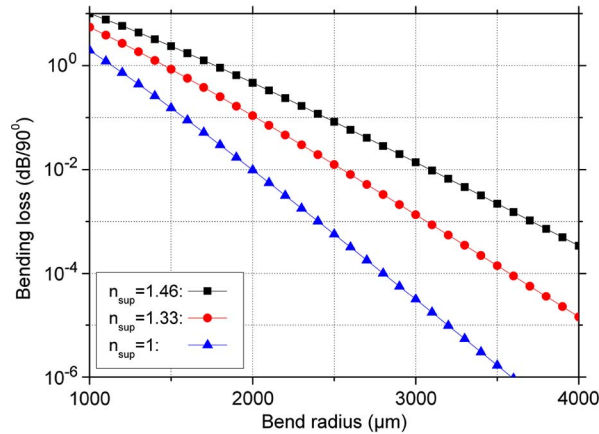


Fig. 7. Bending loss as function of radius for air, water, and silica as the superstrate, for core thickness 150 nm, rib height 5 nm, rib width 2  $\mu$ m, and TE-polarization.

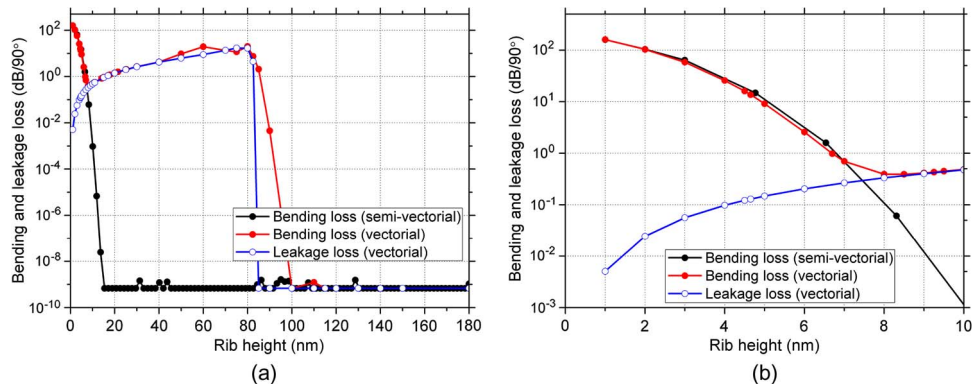


Fig. 8. Bending loss and leakage loss of the fundamental TM mode versus rib height for a core thickness of 180 nm. The full range from 1 nm rib height to strip waveguide (rib height = core height) is shown in (a), while (b) shows the results for shallow rib waveguides only. The bend radius is 1 mm, and the rib width is 2  $\mu$ m.

height of 8 nm, leakage loss becomes the dominating factor and the bending loss increases as the rib height increases further up to 80 nm. For a rib height of 80 nm, leakage loss ceases to exist as the minority field component is now guided. As a consequence, bending losses decrease very sharply to the numerical noise level. For a rib height of more than 80 nm, the waveguide thus behaves as a strip waveguide. Fig. 8 also shows the bending loss calculated with the semi-vectorial method, which does not take leakage loss into account. Thus, the bending loss found with the semi-vectorial method is correct for rib heights less than 8 nm and larger than 80 nm, when leakage loss is not dominating. However, from 8 nm to 80 nm rib height, the semi-vectorial method does not work for TM-polarization as leakage loss is the dominating factor.

In Fig. 9, bending losses are shown as function of core thickness for TE- and TM-polarization and for three rib heights, again for fixed radius and rib width. Some of the combinations of core thickness and rib height in the graph will give multimode waveguides according to Fig. 2. The bending losses have a minimum for a core thickness of approximately 90 nm and 180 nm for TE- and TM-polarization, respectively. For small core thicknesses, the waveguides are approaching cut-off and bending losses increase. For large core thickness, the rib height relative to the core thickness,  $h_r/H$ , decrease, again making bending losses increase. The sum of these effects thus have a minima for 90 and 180 nm. The bending losses decrease fast with increasing rib height, as expected as the mode gets better guided. The dependency on rib height is particularly pronounced for the core thicknesses giving minimum losses, i.e., 90 nm

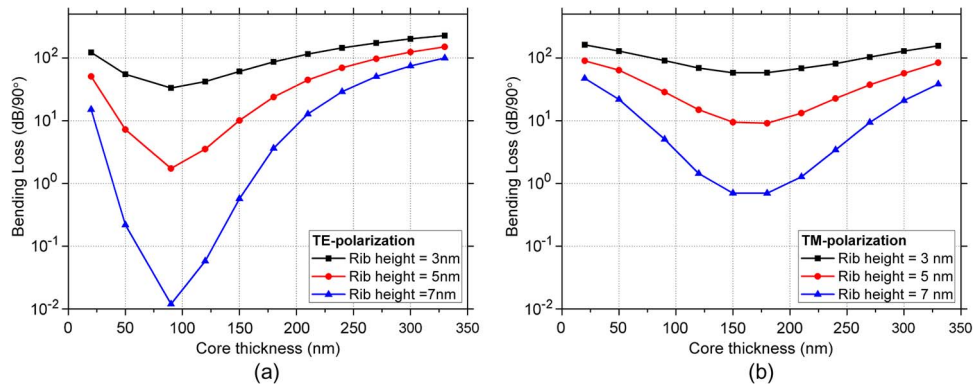


Fig. 9. Bending loss as function of core thickness for three rib heights and for (a) TE- and (b) TM-polarization. The bend radius is 1 mm, and the rib width is  $2 \mu\text{m}$ .

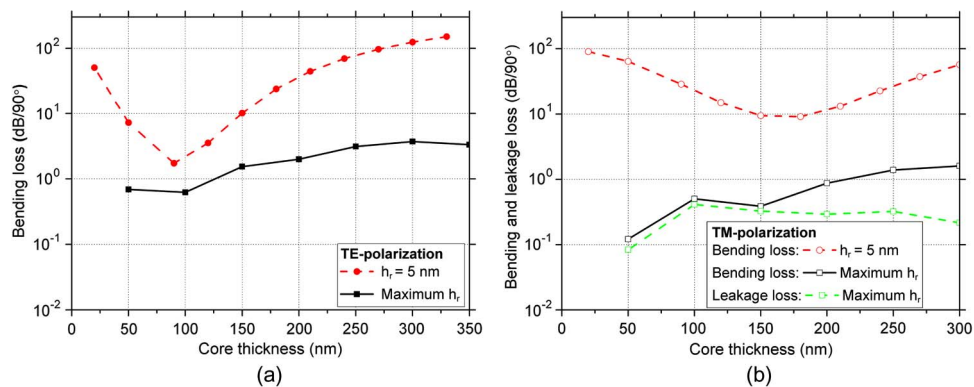


Fig. 10. Bending loss for (a) TE- and (b) TM-polarization as function of core thickness. Red broken lines are for a fixed rib height of  $h_r = 5 \text{ nm}$ , while black solid lines are for the maximum rib height giving single mode waveguides for the given core thickness (see Fig. 2).

and 180 nm for TE- and TM-polarizations, respectively. Note that for the rib heights considered in Fig. 9, leakage loss is not the dominating factor for TM-polarization according to Fig. 8.

The dependency of bending losses on rib height is further explored in Fig. 10. The bending losses are shown (black lines) for a rib height equal to the single-mode limit given in Fig. 2. This is thus the maximum rib height, giving the best guiding, that maintains the waveguide single-mode for a given core thickness and polarization. For comparison, bending losses for a fixed rib height of 5 nm are included. The picture given by the maximum rib heights is somewhat different from that given by fixed rib heights. Bending losses decrease relatively slowly with decreasing core thickness down to 50 nm core thickness. The decrease is less pronounced than expected from Fig. 9 and the decrease continues to smaller core thicknesses than the 90 and 180 nm found above. Also, the losses for TE- and TM-polarization show no significant differences. From Fig. 10, it can be concluded that low bending losses can be obtained for the core thicknesses considered (50–300 nm) by optimizing the rib height to the maximum value giving a single-mode waveguide. The improvement in losses between using a fixed rib height and the maximum value can be several orders of magnitude. In the design process, the core thickness and the polarization should thus be decided before the rib height is chosen, with the disadvantage that the waveguide will be optimized for one polarization only. If polarization independent losses are desired, this can be obtained for some combinations of rib height and core thickness, e.g., 5 nm and 155 nm, respectively, according to Fig. 10. Also, a polarization filter that transmits only TE-polarization can be made by choosing a combination giving high bending losses for TM-polarization and low for TE-polarization, e.g., 7 nm rib height and 80 nm core thickness according to Fig. 9. In Fig. 10(b), the leakage loss is also

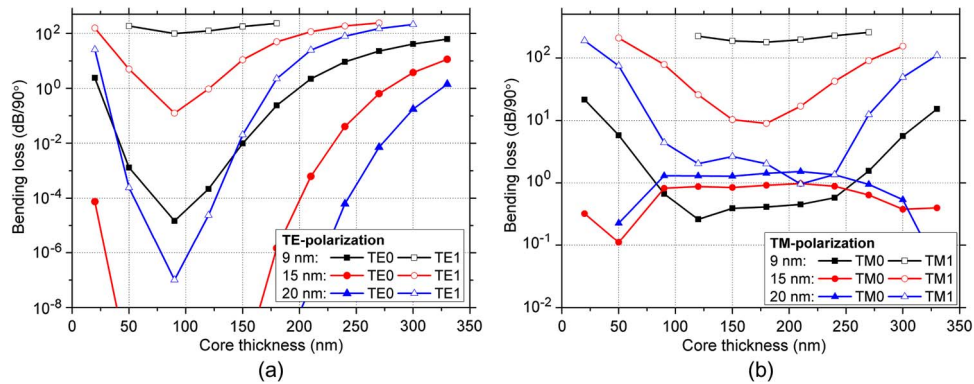


Fig. 11. Bending loss for fundamental and first order mode as function of core thickness for three rib heights for (a) TE-polarization and (b) TM-polarization. The bend radius and the rib width are 1 mm and 2  $\mu\text{m}$ , respectively.

shown, again for a length of  $\pi/2 \times R$ . For a core thickness of 150 nm or less, leakage loss dominates the bending losses, while for larger core thicknesses its contribution decreases.

Up to this point, we have only considered the bending losses of the fundamental mode, which is most common when studying bending losses [16], [17]. In Fig. 11, bending losses are shown for rib heights giving multimode waveguides, with bending losses plotted both for the fundamental mode and the first order mode. For TE-polarization, the bending losses are as much as five orders of magnitude larger for the first order mode than for the fundamental mode. A 90° bend can thus be used as an excellent mode filter, transmitting only the fundamental mode. Also, bending losses for the fundamental mode are decreased by several orders of magnitude by using a rib height giving a multimode waveguide. If a 90° or larger bend is present in the design, it is thus an advantage to use a larger rib height than the single-mode limit shown in Fig. 2, as quasi single-mode operation will still be obtained. For TM-polarization, a similar trend as for TE-polarization is apparent up to a rib height of 9 nm, with significantly smaller losses for the fundamental mode than for the first order mode. For rib heights of 15 and 20 nm, bending loss is dominated by leakage loss according to Fig. 8. As a consequence, the bending loss of the fundamental mode is larger for 15 and 20 nm than for 9 nm in Fig. 11(b), for core thicknesses of 100 to 250 nm. For the same range of core thicknesses, the bending loss of the fundamental and the first order modes are comparable for a rib height of 20 nm. This again demonstrates that leakage loss is an important factor for rib waveguides when using TM-polarization.

#### 4. Conclusion

In this work we have investigated bending losses for shallow rib waveguides. Rib waveguides can be made single-mode by reducing the rib height and the maximum rib height for single-mode waveguides was found as function of the core thickness. The single-mode limit deviates considerably from the standard analytical expression given by [15]. Semi-vectorial and full vectorial methods gave almost identical results for the single-mode limit, both for TE- and TM-polarization. The modes are hybrid and for TM-polarization the minority field components ( $E_x, H_y$ ) are not guided. This causes leakage loss, which the semi-vectorial method does not take into account. It was shown that leakage loss cancels out for some rib widths and increases with rib height, up to a rib height of 80 nm, whereafter the minority field components are guided and the leakage stops.

The small rib height of shallow rib waveguides can reduce propagation losses, but comes at the expense of higher bending losses. The bending losses of a shallow rib waveguide are due to light leaking from the rib and into the adjacent slab waveguide. As leakage loss is present even for straight waveguides for TM-polarization, it is important to use full vectorial simulations except for the smallest rib heights (< 8 nm). We used full vectorial simulations with perfectly matched

layers for all calculations of bending losses. The simulated bending losses increased exponentially with the bend radius, as expected. The influence of the core thickness was found to be more complicated. For a fixed rib height, the bending loss had a minimum for a core thickness of approximately 90 nm and 180 nm for TE- and TM-polarization, respectively. By increasing the rib height to the single-mode limit, the bending losses are in general reduced and relatively low losses can be obtained for both polarizations and all core thickness considered (50–300 nm). The single-mode limit and the bending losses depend on the polarization. A waveguide can thus have low losses and be single-mode for one polarization, while losses are high for the other polarization. Alternatively, it can have low losses for both polarizations, but be multimode for one polarization. By increasing the rib height beyond the single-mode limit, with the waveguide thus becoming multimode, the bending losses are reduced further for the fundamental TE-mode, while the bending losses for the first order mode are high. For TM-polarization, leakage loss is the dominating factor for larger rib heights and bending losses can increase for rib heights larger than about 8 nm (core thickness 180 nm). For a rib height adapted to the core thickness and polarization, a bend can be used as a mode filter transmitting only the fundamental mode. If a large bend is present in the design, e.g., a 90° bend, it may be advantageous to increase the rib height to get lower bending losses for the fundamental mode, while maintaining quasi single-mode operation. As the rib height is the geometrical parameter with largest variation due to the fabrication process of the waveguide, the large losses for the first order mode can also be used as a safety margin. If the rib height is designed to be equal to the single-mode limit but turns out to be higher after it is made, the waveguide will still behave as a single-mode waveguide if large bends are present and if the fabrication error is small.

## Acknowledgement

The authors would like to acknowledge Prof. L. Lechuga and Dr. B. S. Ahluwalia for their valuable suggestions.

---

## References

- [1] D. Duval, A. B. Gonzalez-Guerrero, S. Dante, C. Dominguez, and L. M. Lechuga, "Interferometric waveguide biosensors based on Si-technology for point-of-care diagnostic," in *Proc. SPIE*, 2012, vol. 8431, Art. ID. 84310.
- [2] K. E. Zinoviev, A. B. González-Guerrero, C. Domínguez, and L. M. Lechuga, "Integrated bimodal waveguide interferometric biosensor for label-free analysis," *J. Lightw. Technol.*, vol. 29, no. 13, pp. 1926–1930, Jul. 2011.
- [3] M. Iqbal *et al.*, "Label-free biosensor arrays based on silicon ring resonators and high-speed optical scanning instrumentation," *IEEE J. Sel. Topics Quantum Electron.*, vol. 16, no. 3, pp. 654–661, May/Jun. 2010.
- [4] K. Cottier, M. Wiki, G. Voirin, H. Gao, and R. Kunz, "Label-free highly sensitive detection of (small) molecules by wavelength interrogation of integrated optical chips," *Sens. Actuators B, Chem.*, vol. 91, no. 1–3, pp. 241–251, Jun. 2003.
- [5] J. García-Rupérez *et al.*, "Label-free antibody detection using band edge fringes in SOI planar photonic crystal waveguides in the slow-light regime," *Opt. Exp.*, vol. 18, no. 23, pp. 24 276–24 286, Nov. 2010.
- [6] A. Ymeti *et al.*, "Drift correction in a multichannel integrated optical young interferometer," *Appl. Opt.*, vol. 44, no. 17, pp. 3409–3412, Jun. 2005.
- [7] F. Prieto *et al.*, "An integrated optical interferometric nanodevice based on silicon technology for biosensor applications," *Nanotechnol.*, vol. 14, no. 8, pp. 907–912, Aug. 2003.
- [8] Y. Vlasov and S. McNab, "Losses in single-mode silicon-on-insulator strip waveguides and bends," *Opt. Exp.*, vol. 12, no. 8, pp. 1622–1631, Apr. 2004.
- [9] S. M. Lindecrantz and O. G. Helleso, "Estimation of propagation losses for narrow strip and rib waveguides," *IEEE Photon. Technol. Lett.*, vol. 26, no. 18, pp. 1836–1839, Sep. 2014.
- [10] X. Xu, S. Chen, J. Yu, and X. Tu, "An investigation of the mode characteristics of SOI submicron rib waveguides using the film mode matching method," *J. Opt. A, Pure Appl. Opt.*, vol. 11, no. 1, 2009, Art. ID. 015508.
- [11] M. Webster, R. Pafchek, A. Mitchell, and T. Koch, "Width dependence of inherent TM-mode lateral leakage loss in silicon-on-insulator ridge waveguides," *IEEE Photon. Technol. Lett.*, vol. 19, no. 6, pp. 429–431, Mar. 2007.
- [12] T. G. Nguyen, R. S. Tummidi, T. L. Koch, and A. Mitchell, "Lateral leakage of TM-like mode in thin-ridge silicon-on-insulator bent waveguides and ring resonators," *Opt. Exp.*, vol. 18, no. 7, pp. 7243–7252, Mar. 2010.
- [13] B. Sepúlveda *et al.*, "Optical biosensor microsystems based on the integration of highly sensitive Mach-Zehnder interferometer devices," *J. Opt. A, Pure Appl. Opt.*, vol. 8, no. 7, pp. S561–s566, Jun. 2006.

- [14] R. Soref, J. Schmidtchen, and K. Petermann, "Large single-mode rib waveguides in GeSi-Si and Si-on-SiO<sub>2</sub>," *IEEE J. Quantum Electron.*, vol. 27, no. 8, pp. 1971–1974, Aug. 1991.
- [15] S. P. Pogossian, L. Vescan, and A. Vonsovici, "The single-mode condition for semiconductor rib waveguides with large cross section," *J. Lightw. Technol.*, vol. 16, no. 10, pp. 1851–1853, Oct. 1998.
- [16] D. Dai and S. He, "Analysis of characteristics of bent rib waveguides," *JOSA A*, vol. 21, no. 1, pp. 113–121, Jan. 2004.
- [17] M. Krause, H. Renner, and E. Brinkmeyer, "Polarization-dependent curvature loss in silicon rib waveguides," *IEEE J. Sel. Topics Quantum Electron.*, vol. 12, no. 6, pp. 1359–1362, Nov./Dec. 2006.
- [18] F. Prieto *et al.*, "Integrated Mach-Zehnder interferometer based on arrow structures for biosensor applications," *Sens. Actuators B, Chem.*, vol. 92, no. 1/2, pp. 151–158, Jul. 2003.
- [19] S. Lindecrantz, F. T. Dullo, B. S. Ahluwalia, and O. G. Hellesø, "Sensitivity of Mach-Zehnder interferometer for dissolved gas monitoring," in *Proc. SPIE*, 2014, vol. 8988, Art. ID. 898818.